

Experimental and theoretical study of dynamic bend angle in the explosive welding process

Bir Bahadur Sherpa^{1,2,3}  · Pal Dinesh Kumar² · Abhishek Upadhyay² · Sandeep Kumar² · Arun Agarwal² · Sachin Tyagi^{1,3}

Received: 9 August 2020 / Accepted: 3 January 2021 / Published online: 21 January 2021
© The Indian Institute of Metals - IIM 2021

Abstract Dynamic bend angle (β) is an important parameter that should satisfy the range defined by the weldability window for successful joining in the explosive welding process. In this manuscript, we studied the dynamic bend angle (β) for the newly developed low velocity of detonation explosive welding (LVEW) process theoretically and then experimentally with the help of flash X-ray radiography (FXR) technique. The FXR system captured the real-time image of the event where proper explosive welding process with clear flight shape and appropriate collision bend angle was observed. The FXR results were in good agreement with numerically calculated β values and demonstrated the suitability of LVEW process for joining of dissimilar metal plates. This was further justified by phased array-based ultrasonic testing (PAUT) results where complete bonding area with slight non-bonded area was observed across the edges of the welded metal plate.

Keywords Dynamic bend angle · LVEW process · PAUT · Weldability window · FXR

1 Introduction

To study the dynamic behaviour of a high velocity impact process especially in the field of detonation and explosion, flash X-ray radiography (FXR) technique is considered as one of the competent diagnostic technique. There are many conventional diagnostic techniques to capture the events such as schlieren photography, high-speed photography, laser interferometry etc., but they are not suitable for capturing the inside view of the events (point of interest) as during explosion many things occur simultaneously in microseconds. FXR has the capability to penetrate through the events and capture the dynamic phenomenon despite the hindrances such as luminescent gas cloud, kinetic flash as well as the formation of debris during explosion [1, 2]. FXR diagnostic technique has been used by many researchers for analysis of high-velocity impact process, high-speed thermal jets, debris clouds as well as dwell phenomena in the ballistic event [1, 3–6].

These advantageous features of the FXR diagnostic technique can also be applied to study the high impact phenomenon of the explosive welding process. In the explosive welding process, flyer plate velocity (V_p) and the dynamic bend angle (β) determine the pressure and the shear stress at the weld area (collision zone) [7]. This combined pressure and shear stress result in the development of a jetting phenomenon, which is one of the important criteria in explosive welding process for joining to take place and directly depends on the β angle [7–9]. During the collision process, jetting phenomenon occurs at the collision point as a result of high impact pressure generated from explosion effects. It is a small jet of softened metal which is formed at the collision front which thoroughly cleans the mating surfaces leaving behind virgin surfaces free from contaminants. As a result, the two

✉ Bir Bahadur Sherpa
sherpa7419@gmail.com

¹ Academy of Scientific and Innovative Research (AcSIR), Ghaziabad-201002, India

² DRDO-Terminal Ballistics Research Laboratory (TBRL), Sector-30, Chandigarh 160030, India

³ CSIR-Central Scientific Instruments Organisation (CSIO), Sector-30, Chandigarh 160030, India

mating surfaces can interact at the atomic level during the collision process and form a strong metallurgical bond. In the explosive welding process, there are two types of the set-up, i.e. inclined (plates to be welded are kept at a particular angle) set-up as shown in Fig. 1a and the parallel set-up (plates are kept parallel to each other) as shown in Fig. 1b [10, 11] and β is formed between the flyer and the base plate. There is a critical boundary in explosive welding after which joining is not possible if the dynamic

bend angle is less than the minimum limit. Bahrani and Crossland studied dynamic bend angle for the explosive welding process and observed that for a proper bond to occur β should lie between $2\text{--}3^\circ$ and 31° [12, 13]. While Lysak and Kuzmin experimentally observed that the transformation to waveless joint not only depends on collision velocity (V_c) but also influenced by β [14]. During the explosive welding process, collision point velocity (V_c) and plate velocity (V_p) should be less than that of the

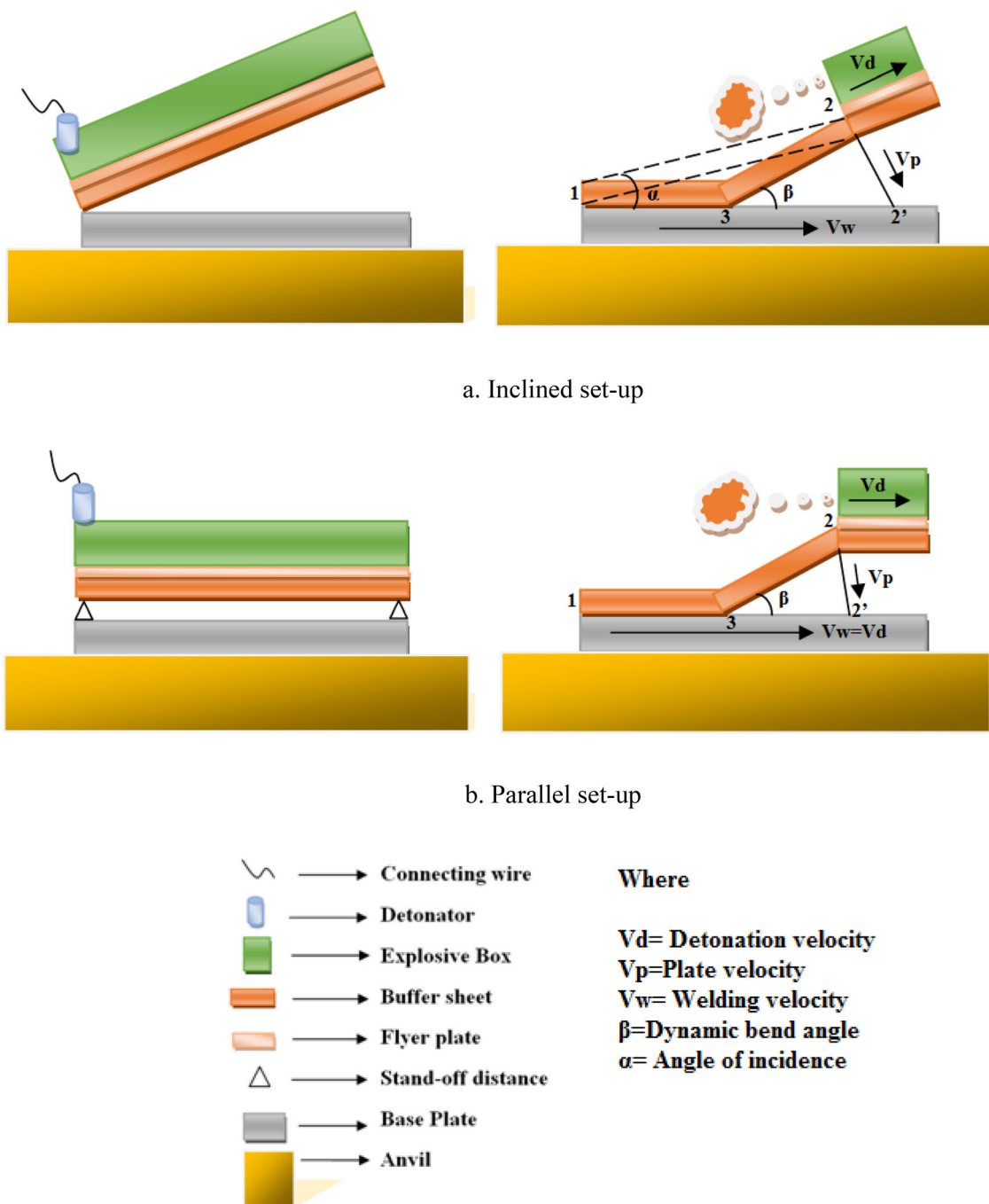


Fig. 1 Explosive welding process set-up: **a** Inclined, **b** Parallel

velocity of sound in either of the welded material. Where V_c governs the time available for bonding and V_p is the velocity with which flyer plate impact on the base plate due to explosion pressure. Using V_c and V_p , dynamic bend angle (β) is calculated numerically. β and V_p have a direct relationship and an increase in V_p will result in enhanced kinetic energy loss during the collision process, as a result, defected weld is formed. Moreover, a jetting phenomenon which is one of the main criteria for welding is also effected by β . Therefore, there is a need to study dynamic bend angle as it should be in a defined range for a smooth weld to form. Dynamic bend angle is one of the critical parameters, and limited work has been reported related to detailed study of β (experimentally). Considering this, the present work aims to study the dynamic bend angle (β) for a newly developed low velocity of detonation explosive welding (LVEW) process ($V_d < 2000$ m/s) [15]. Here, we have employed flash X-ray radiography (FXR) technique to have a clear and real-time visualization of explosive welding which is a microsecond phenomenon and difficult to observe with naked eyes. FXR films were used to measure dynamic bend angle (β) and matched with theoretically calculated values. To check the integrity of the bond quality after welding, an advanced form of ultrasonic testing (UT) namely phased array-based ultrasonic testing (PAUT) was employed.

2 Materials and Methods

2.1 Materials

In this work, aluminium (Al) plate with dimensions of 300 mm × 30 mm × 5 mm was used as flyer plate and low carbon steel (LCS) plate with 300 mm × 30 mm × 21 mm as a base plate. The two plates were explosively welded using low velocity of detonation explosive welding (LVEW) process with $V_d < 2000$ m/s in the parallel set-up. The study was executed both in static and dynamic conditions.

2.2 Static Experiments

In a static experiment, no detonation happens. It is usually performed to verify the actual distance required between source to the event (SE) and event to film (EF) for dynamic study. The experimental set-up for the static study is shown in Fig. 2a. The set-up consists of 480 kV flash X-ray tube, event and the X-ray film. In Fig. 2a, top view of the set-up is shown where the event (explosive welding set-up) is placed between the source (flash X-ray tube) and the film.

2.3 Dynamic Experiments

To study the dynamic bend angle in the explosive welding process, a dynamic experiment was conducted, and the schematic is shown in Fig. 2b. For this, three different X-ray tubes and X-ray films were used. The dynamic experiment was carried out on the explosive welding process. In Fig. 3, complete experimental set-up for dynamic experiment consisting of source (flash X-ray tube), event (explosive welding set-up) & film is shown, while Fig. 3b shows the front view of the event set-up with X-ray film and Fig. 3c display the close view of event set-up. During the experiment, X-ray tubes were triggered at three different time intervals, i.e. 80 μ s, 120 μ s & 150 μ s to analyse the dynamic behaviour of the LVEW process.

2.4 Dynamic Bend Angle (β)

In the explosive welding process, when the flyer plate comes in contact with the base plate at a very high-pressure dynamic bend angle is formed. The dynamic bend angle should be in described limits for successful joining (within weldability window). Abrahamson showed that collision velocity can be related to dynamic bend angle as shown in Eq. 1, while plate velocity is directly related to dynamic bend angle as expressed by Eq. 2 [16].

$$V_c = \frac{\beta}{10} + 5.5 \quad (1)$$

$$V_p = 2V_c \sin \frac{\beta}{2} \quad (2)$$

where V_p : plate velocity & V_c : collision velocity.

To get a good bond, there should be a balanced plate velocity, so that the flyer plate can get bonded to the base plate. Where, high V_p (upper limit) may lead to joining with several defects such as intermetallic formation, cracks, and voids. In the explosive welding process, the jetting phenomenon is one of the most important criteria which indicates the formation of a good bond. For jetting to occur, the minimum value of the dynamic bend angle also called critical bend angle (β_c) is required which is calculated using Eq. 3.

$$\beta_c = k_1 \sqrt{\frac{H}{\rho V_c^2}} \quad (3)$$

where H: Vickers hardness, ρ = density, $k_1 = 0.6$ (high-quality surface) & 1.2 (rough/imperfectly cleaned surface).

In the explosive welding process for proper weld condition, the dynamic bend angle should lie between 2–3° and 31° [13]. In this regard, we have theoretically calculated dynamic bend angle (β) and the critical dynamic bend angle (β_c) using Eq. 2 and 3. Here, detonation velocity

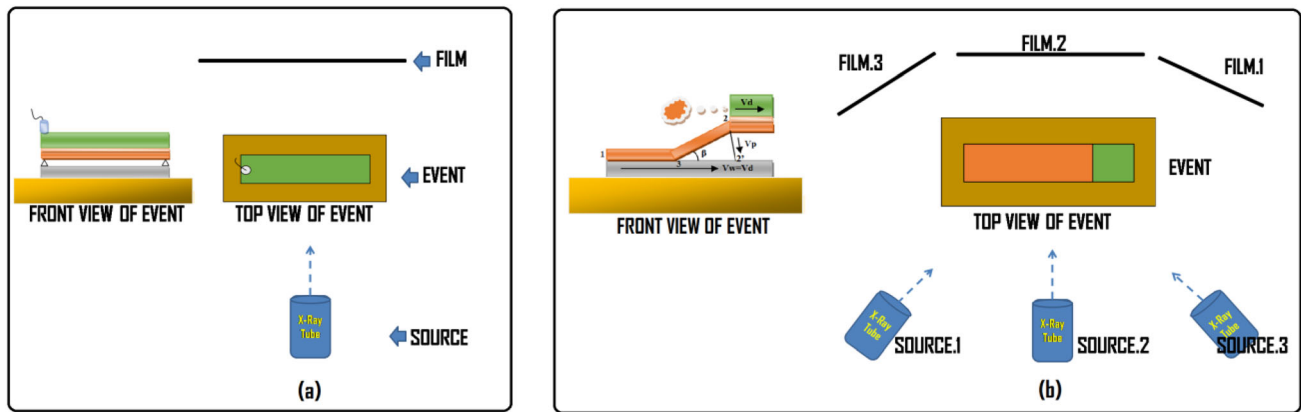


Fig. 2 a Schematic of FXR set-up for static experiments, b Schematic of FXR setup for dynamic experiments

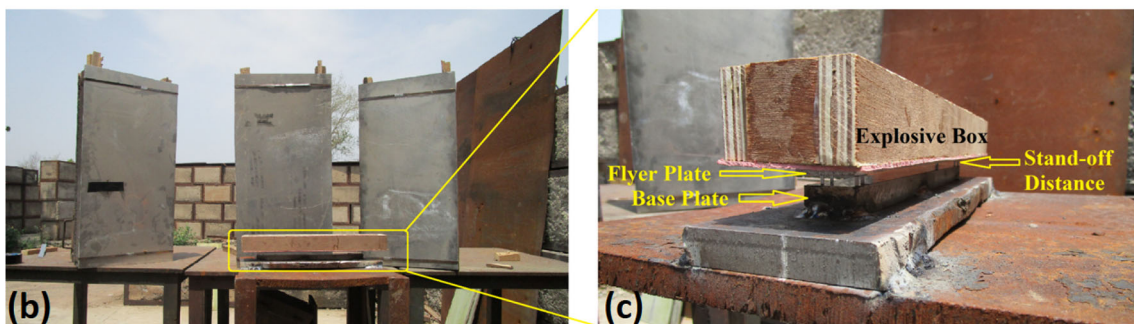
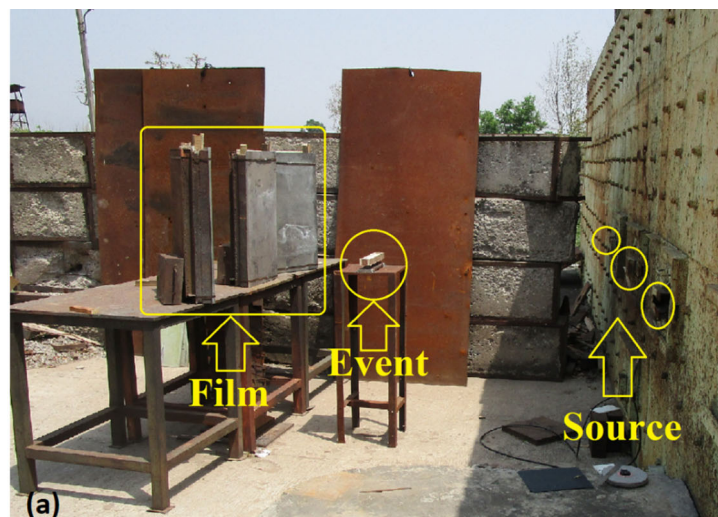


Fig. 3 Experimental set-up for dynamic experiment: a complete set-up for flash X-ray radiography, b front view of the event set-up with X-ray film, c close view of event set-up

(VoD = Vc) 1607 m/s, H: 40 HV1 and flyer plate velocity (Vp) 388 m/s were used. The obtained values of β and β_c are 13.9° and 8.2° , respectively.

2.5 Non-Destructive Testing (NDT)

Non-destructive testing (NDT) was performed through PAUT (Sonatest) with the configuration of 16:64 having

5 MHz probe frequency. This technique is an advanced form of ultrasonic testing (UT) and works on the simple principle of sound energy (i.e. transmittance and reflection of the sound waves). In this process, the sound waves are passed (transmitted) through the material being inspected. The reflection of the waves from the material provides information about the debonded area as the waves get

reflected wherever any kind of discontinuity is observed [17, 18].

3 Results and Discussion

3.1 Flash X-Ray Radiography

Figure 4a,b shows Al & LCS plates before and after the experiment, respectively. Visual inspection of the welded specimen demonstrates complete bonded surface. The static record of the event is shown in Fig. 5a in which separation of the two plates can be seen clearly by a stand-off distance and for more visualization, schematic set-up is shown in the left side of the static event result. These observations provide a clear idea about the event being suitable for dynamic experiment in terms of the distance between sources to event & event to film. The experimental details of the distance used in flash X-ray radiography are shown in Table 1.

The FXR films of the explosive welding process at different time intervals i.e. at 80 μs and 120 μs are shown in Fig. 5b, c. Upon detonation, the flow of explosive products can be seen moving throughout the flyer plate, which is a clear indication of the explosive been initiated during the explosive welding process. In the experiment, two films at time 80 μs and 120 μs have been initiated appropriately but unfortunately, the third record of 150 μs is not obtained due to over-exposure of the film. In both the films, dynamic bend angle (β) is revealed while the collision point moves smoothly in the direction of event propagation. In both the cases almost parallel gap can be observed during the collision process between the flyer & the base plate with a constant dynamic angle [19]. Figure 5d shows the schematic representation of the dynamic bend angle in which $V_c = V_d$, as in parallel set-up, collision velocity (V_c) is considered equal to detonation

velocity (V_d) [20]. The dynamic bend angle, when determined experimentally in above explosive welding trial, using flash radiography, comes out to be 12–13°. Which is very close to the theoretically calculated dynamic bend angle value and a slight difference in value may have resulted due to the non-ideal nature of the explosive. This result confirms that the calculated welding parameters based on which the above experiment was carried out are in good agreement with the actual values. The remarkable feature of this diagnostic evaluation is that, the critical parameter (dynamic bend angle) has been achieved which has led to uniform & sound joining as confirmed by PAUT machine.

3.2 Analysis of the Weldability Window

The concept of the weldability window was first introduced to check whether bonding will occur or not under miscellaneous welding conditions. The weldability window can be plotted between any two preferred parameters [21]. Earlier Cowan et al. developed a weldability window between flyer plate velocity and flyer mechanical properties [22]. Presently, the most used and well-known method to develop weldability window is based on the idea of Deribas et al. where they developed weldability window using dynamic bend angle in ordinates and collision point velocity in abscissa as shown in Fig. 6. [23]. Weldability window is usually comprised of straight and curved boundaries defining left, right, lower, and upper limits along with the minimum and maximum bend angle and critical angle required for jetting phenomenon. The first boundary (left limit) describes the transition condition required to achieve a wavy interface [22]. Second boundary (right limit) discusses the formation of an interfacial jet which is necessary for weld to occur at the collision point [24]. The third boundary (lower limit) expresses the minimum energy required at the collision point to promote plastic deformation [25], while the fourth boundary (upper limit) defines the maximum energy which is needed to avoid the interfacial melting [26]. Figure 6 illustrates the weldability window in which V_p values corresponding to both the theoretical and experimental values of β are presented. Where V_p (Num.) is the plate velocity obtained through numerical calculations of β and V_p (Expt.) is the plate velocity range obtained through FXR calculations. From Fig. 6, it can be witnessed that the welding conditions used are near the lower boundary. In explosive welding, the lower boundary is more preferable as it leads to minimum collision velocity and strong weld joints [14]. Welding conditions near the lower limit of the weldability window will help to form defect-free joints as the maximum possibilities of defects arise when more energy is involved. This was also discussed by M. Ahasan Habib



Fig. 4 Al-LCS plates: **a** before experimental trial, **b** after experimental trial

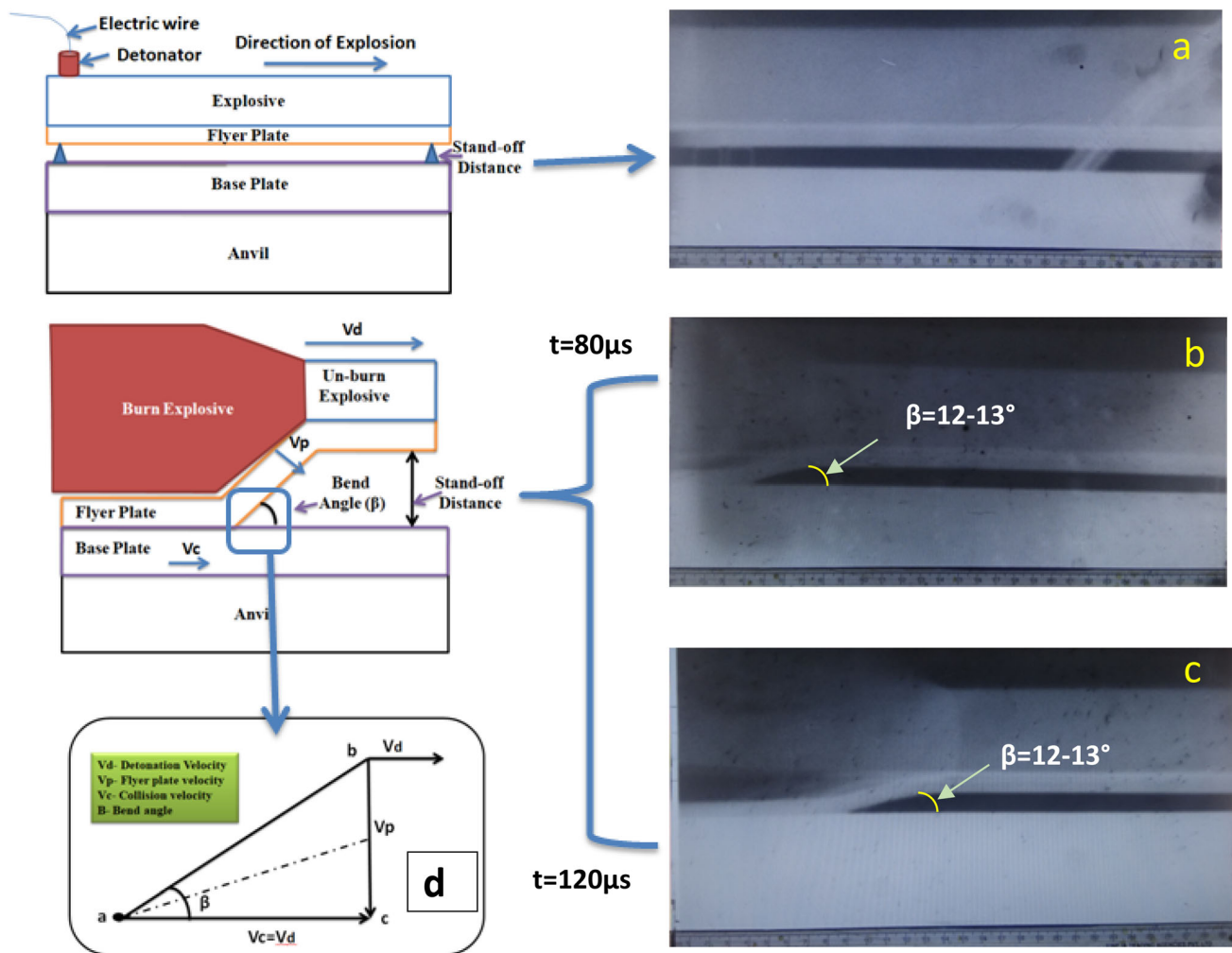


Fig. 5 Flash X-ray radiography results: **a** Static event results, **b** Dynamic event results at $t = 80 \mu\text{s}$, **c** Dynamic event results at $t = 120 \mu\text{s}$, **d** Pictorial representation of the β angle

Table 1 Experiment details of Flash X-ray radiography done using three X-ray tubes

Sr. no	Distance of source to event (cm)	Distance of event to film (cm)
01	180	90
02	235	125
03	240	110

et al. in underwater explosive welding where they suggested that by decreasing the pressure, welding conditions were enhanced and also the formation of the thick molten zone was eliminated [27]. Therefore, the welding conditions applied in this experiment has brought good results in terms of bond formation, which was further verified using phased array-based ultrasonic testing (PAUT).

3.3 Phased Array Ultrasonic Testing (PAUT)

Experimental results show that explosive welding of Al/LCS is successfully achieved through LVEW process. The bimetallic Al/LCS plate is subjected to PAUT, which is an advanced form of ultrasonic testing for inspection of welded plate [28]. In this process, water is used as a couplant

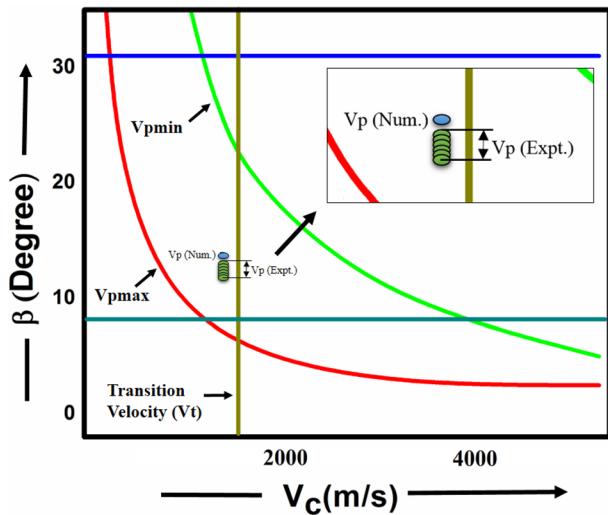


Fig. 6 Weldability window showing V_p obtained through FXR and numerical calculations

to ensure continuity of medium for sound waves to travel from probe to the welded surface. The A-scan results of explosively welded Al/LCS plates for bonded portion are shown in Fig. 7a. The first peak with low intensity has been reflected from interface, which shows that the sound waves have passed through the interface and due to absence of air

gaps; the energy reflected is low resulting in low-intensity peak. While the second peak from the back wall shows that the sound waves have travelled across the welded material [29]. Similarly, the debonded area is shown in Fig. 7b where the single peak is observed, which indicates that the sound waves have not gone through the interface and got reflected from the interface itself due to the presence of air gaps. This single high-intensity peak is a clear indication of the debonded area. The complete pictorial views of the welded Al/LCS bimetallic plate is shown in Fig. 7c which shows that maximum area is welded with some portion of around 5–10 mm at the outer edges on all sides is debonded, which is also in agreement of the work done by S.A.A. Akbari-Mousavi et al. [30], NV Rao et al. [31] & P. Mastanaiah et al. [32].

4 Conclusion

In this research work, Al and LCS plates were explosively welded, and simultaneous diagnostic analysis was performed through flash X-ray radiography technique. In addition to this, PAUT test was used for inspection of the bimetallic plate. The study revealed certain interesting observations which have been summarized as follows:

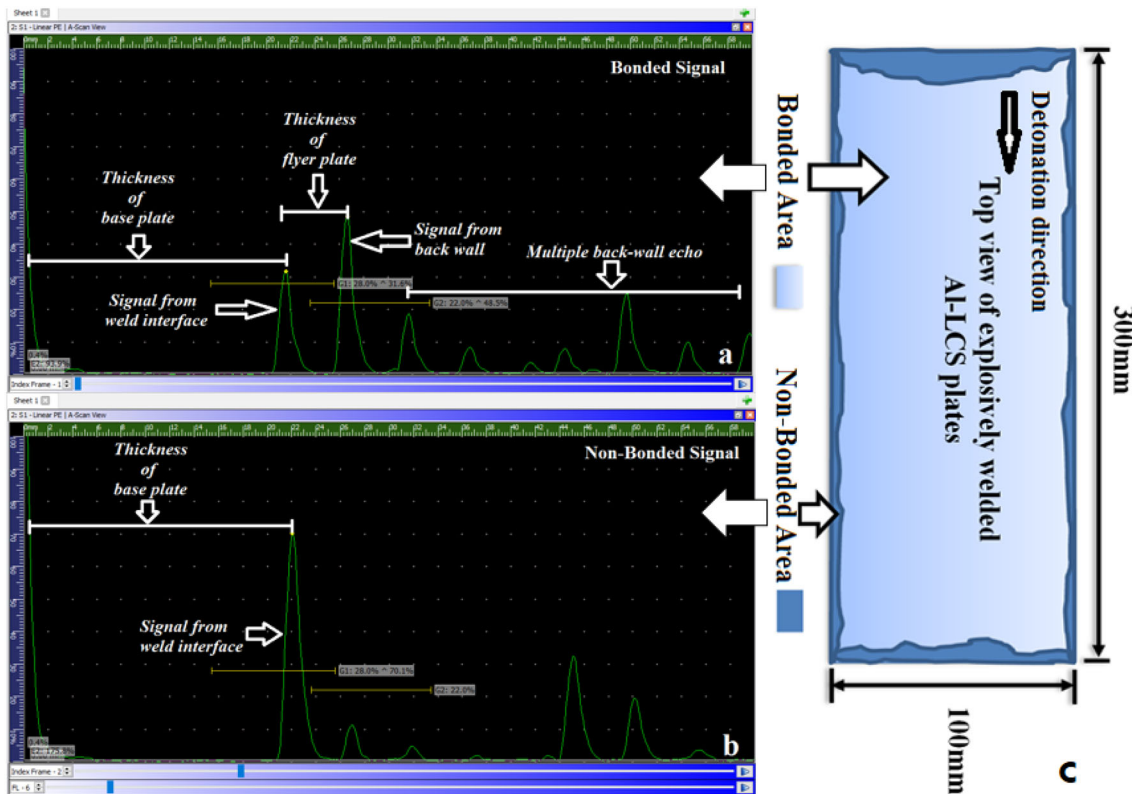


Fig. 7 PAUT results: **a** A-scan for bonded portion, **b** A-scan for the non-bonded portion, **c** complete representation of explosively welded Al/LCS plate

- To analyze the dynamic behaviour of the explosive welding process, flash X-ray radiography is one of the best suitable diagnostic techniques. Flash X-ray radiography images taken at different time intervals of 80 μ s & 120 showed proper explosive welding process with clear flight shape and formation of a collision bend angle, but due to overexposure of the film, the third record of 150 μ s was not obtained.
- The theoretically calculated value of dynamic bend angle (β) was in good agreement with experimentally calculated one. Only a slight difference in value was observed, which may have resulted due to the non-ideal nature of the explosive.
- PAUT of welded Al/LCS plates was performed, in which it passed the test with no significant defects. Debonded area was observed at the outermost edges from all the sides.
- The FXR and PAUT results demonstrated the suitability of LVEW process for joining of dissimilar metal plates.

Acknowledgement The support from the Terminal Ballistics Research Laboratory is highly acknowledged. Authors are very thankful to Dr Manjit Singh, Director, TBRL, Sec 30, Chandigarh, all the scientists of Zone-IV, EED, M.T., and Workshop of TBRL for their valuable support.

References

1. Ramudu, B.V., C.J. Reddy, and V. Madhu, *Flash X-ray radiography technique to study the high velocity impact of soft projectile on E-glass/epoxy composite material*. Defence Technology, 2019. **15**(2): p. 216-226.
2. Helberg, P., K. Michael, and K. Thoma. *Flash x-ray computed tomography for applications in high-speed dynamics*. in *9th European Conf. Non-Destructive Testing, Berlin*. 2006.
3. Mizusako, F., et al., *Flash x-ray radiography using imaging plates for the observation of hypervelocity objects*. Review of scientific instruments, 2005. **76**(2): p. 025102.
4. Strassburger, E., et al., *Flash X-ray cinematography analysis of dwell and penetration of small caliber projectiles with three types of SiC ceramics*. Defence Technology, 2016. **12**(3): p. 277-283.
5. Tamura, H., Y. Tanaka, and F. Saito, *Quantitative analysis of debris from SiC-fiber-reinforced aluminum-alloy targets impacted by spherical projectiles*. International journal of impact engineering, 2011. **38**(8-9): p. 686-696.
6. Thoma, K., P. Helberg, and E. Strassburger. *Real time-resolved flash X-ray cinematographic investigation of interface defeat and numerical simulation validation*. in *23rd Int'l Symposium on Ballistics, Tarragona, Spain, ADPA*. 2007.
7. Wang, X., et al., *Numerical study of the mechanism of explosive/impact welding using smoothed particle hydrodynamics method*. Materials & Design, 2012. **35**: p. 210-219.
8. Mousavi, S.A. and S. Al-Hassani, *Finite element simulation of explosively driven plate impact with application to explosive welding*. Materials & Design, 2008. **29**(1): p. 1-19.
9. Mousavi, A.A., S. Burley, and S. Al-Hassani, *Simulation of explosive welding using the Williamsburg equation of state to model low detonation velocity explosives*. International journal of impact engineering, 2005. **31**(6): p. 719-734.
10. Sherpa, B.B., et al., *Study of the Explosive Welding Process and Applications*. Advances in Applied Physical and Chemical Sciences-A Sustainable Approach, 2014: p. 33–39.
11. Sherpa, B.B., et al., *Neuro-Fuzzy Technique for Micro-hardness Evaluation of Explosive Welded Joints*. Transactions of the Indian Institute of Metals, 2020. **73**(5): p. 1287-1299.
12. Zhou, Q., J. Feng, and P. Chen, *Numerical and experimental studies on the explosive welding of tungsten foil to copper*. Materials, 2017. **10**(9): p. 984.
13. Crossland, B. and A. Bahrani, *Fundamentals, of explosive welding*. Contemporary Physics, 1968. **9**(1): p. 71-87.
14. Lysak, V. and S. Kuzmin, *Lower boundary in metal explosive welding. Evolution of ideas*. Journal of Materials Processing Technology, 2012. **212**: p. 150–156.
15. Sherpa, B.B., et al., *Low Velocity of Detonation Explosive Welding (LVEW) Process for Metal Joining*. Propellants, Explosives, Pyrotechnics, 2020. **45**(10): p. 1554-1565.
16. Abrahamson, G.R., *Permanent periodic surface deformations due to a traveling jet*. Journal of Applied Mechanics, 1961. **28**(4): p. 519-528.
17. Pugalendhi, P. and D. Veeraru. *Use of Phased Array Ultrasonic Testing (PAUT) & Time Of Flight Diffraction (TOFD) in Lieu of Radiography Testing on ASME U Stamp Pressure Vessel fabrication Projects*. in *Singapore International NDT Conference & Exhibiton*. 2013.
18. Caravaca, D., C. Bird, and D. Kleiner, *Ultrasonic phased array inspection of electrofusion joints in polyethylene pipes*. Insight-Non-Destructive Testing and Condition Monitoring, 2007. **49**(2): p. 83-86.
19. Tabatabaee Ghomi, M., *Impact wave process modeling and optimization in high energy rate explosive welding*. 2009, Mälardalens högskola.
20. Andreevskikh, L.A., et al., *Explosive mixture for explosive welding of thin foils*. Propellants, Explosives, Pyrotechnics, 2011. **36**(1): p. 48-50.
21. Ribeiro, J., R. Mendes, and A. Loureiro. *Review of the weldability window concept and equations for explosive welding*. in *Journal of Physics: Conference Series*. 2014. IOP Publishing.
22. Cowan, G., O. Bergmann, and A. Holtzman, *Mechanism of bond zone wave formation in explosion-clad metals*. Metallurgical and Materials Transactions B, 1971. **2**(11): p. 3145-3155.
23. Deribas, A., V. Simonov, and I. Zakcharenko. *Investigation of explosive welding parameters for arbitrary combinations of metals and alloys*. in *Proc. 5th Int. Conf. on High Energy Rate Fabrication*. 1975. University of Denver Denver, CO.
24. Walsh, J., R. Shreffler, and F. Willig, *Limiting conditions for jet formation in high velocity collisions*. Journal of Applied Physics, 1953. **24**(3): p. 349-359.
25. Deribas, A. and I. Zakharenko, *Surface effects with oblique collisions between metallic plates*. Combustion, Explosion and Shock Waves, 1974. **10**(3): p. 358-367.
26. Wittman, R. *Use of explosive energy in manufacturing metallic materials of new properties*. in *Proceedings of the Second International Symposium, Marianski Lazne, Czechoslovakia*. 1973.
27. Habib, M.A., et al., *Cladding of titanium and magnesium alloy plates using energy-controlled underwater three layer explosive welding*. Journal of Materials Processing Technology, 2015. **217**: p. 310-316.
28. Huggett, D., et al., *Phased array ultrasonic testing for post-weld and online detection of friction stir welding defects*. Research in Nondestructive Evaluation, 2017. **28**(4): p. 187-210.

29. Sherpa, B.B., et al. *Interface Study of Explosive Welded AL-Steel Joint Using Ultrasonic Phased Array Technique*. in *31st International Symposium on Ballistics*. 2019.
30. Akbari-Mousavi, S., L. Barrett, and S. Al-Hassani, *Explosive welding of metal plates*. Journal of materials processing technology, 2008. **202**(1-3): p. 224-239.
31. Rao, N.V., et al., *Influence of hot rolling and heat treatment on structure and properties of HSLA steel explosively clad with austenitic stainless steel*. Materials Science and Technology, 2009. **25**(11): p. 1387-1396.
32. Mastanaiah, P., et al., *An investigation on microstructures and mechanical properties of explosive clad C103 niobium alloy over C263 nimonic alloy*. Journal of Materials Processing Technology, 2014. **214**(11): p. 2316-2324.

Publisher's Note Springer Nature remains neutral with regard to jurisdictional claims in published maps and institutional affiliations.